University, Nagoya, Japan.
[1]C. Herring and C. Kittel, Phys. Rev. 81, 869 (1951); C. Herring, Phys. Rev. 87, 60 (1952).
[2]T. Izuyama and R. Kubo, J. Appl. Phys. Suppl. 35, 1074S (1964).
[3]T. Izuyama (to be published).
[4]W. Marshall, Proceedings of the Eighth International Conference on Low-Temperature Physics, London, 1962 (Butterworths Scientific Publications, Ltd., London, 1962).
[5]T. Nakamura, Phys. Rev. Letters 12, 279 (1964).
[6]T. Izuyama, Progr. Theoret. Phys. (Kyoto) 23, 969 (1960).
[7]F. J. Dyson, Phys. Rev. 102, 1217 (1956).
[8]K. Sawada, Phys. Rev. 106, 372 (1957); R. Brout, Phys. Rev. 108, 515 (1957); K. Sawada, K. A. Brueckner, N. Fukuda, and R. Brout, Phys. Rev. 108, 507 (1957).

INTERPRETATION OF CO_2 OPTICAL MASER EXPERIMENTS

C. K. N. Patel
Bell Telephone Laboratories, Murray Hill, New Jersey
(Received 27 April 1964)

Optical maser action on a number of rotational transitions of the $\Sigma_u^+ - \Sigma_g^+$ vibrational band of CO_2 has been recently reported.[1] The maser lines were identified as the rotational transitions from $P(12)$ to $P(38)$ of the 0 0^01 - 1 0^00 band and from $P(22)$ to $P(34)$ of the 0 0^01 - 0 2^00 band. We wish to give here a simple theoretical treatment which allows us to interpret the results and especially the fact that no R-branch transitions were seen in maser oscillation. The treatment satisfactorily explains the results and leads to an interesting conclusion that for the vibrational-rotational transitions, optical maser action can be obtained on the P-branch transitions even when no inversion exists between the total population densities in the two vibrational states.

Figure 1 shows pertinent parts of the energy level diagram of CO_2 (Herzberg[2]). The rotational levels belonging to each of the vibrational states are not shown for the sake of simplicity. The upper maser level (for both the bands) $\Sigma_u^+(0\ 0^01)$ is optically connected to the ground state $\Sigma_g^+(0\ 0^00)$ of CO_2 through strongly allowed transitions at 2349.3 cm^{-1}. The lower laser levels $\Sigma_g^+(1\ 0^00$ and $0\ 2^00)$ both decay to the $\Pi_u(0\ 1^10)$ levels through radiative transitions at 720.5 and 618.1 cm^{-1}, respectively, and these transitions are reported to be of medium strength (reference 2). The molecules in the $\Pi_u(0\ 1^10)$ levels decay through strongly allowed transitions at 667.3 cm^{-1} to the ground state of CO_2. Thus the maser scheme looks like a four-level system. The probable excitation and decay processes are shown in Fig. 1 with their appropriate strengths as obtained from reference 2. Alternate lines in the rotational spectrum of $\Sigma_u^+ - \Sigma_g^+$ bands of CO_2 are missing because of symmetry considerations for the linear and symmetric molecule CO_2. Also, the Q-branch– i.e., $\Delta J = 0$–transitions are forbidden since both the upper and the lower levels have $l = 0$.

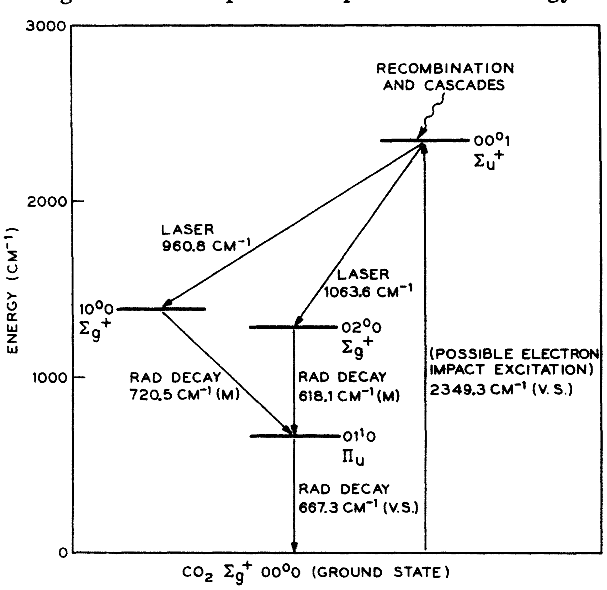

FIG. 1. Pertinent part of energy level diagram of CO_2 showing the maser transitions and other optical transitions with their respective strengths (reference 2).

Now consider a simplified model of a vibrational level in which the rotational level populations are described by a Boltzmann distribution at a temperature T. It can be shown[2] that for a linear and symmetric molecule like CO_2,

$$N_J \approx N(hcB/kT) g_J e^{-F(J)hc/kT} \quad \text{for } hcB/kT \ll 1, \quad (1)$$

where N_J is the population density of the Jth rotational level, $N = \sum_J N_J$, h = Planck's constant, c = velocity of light, B = rotational constant for the particular vibrational level, k = Boltzmann's constant, g_J = statistical weight for the Jth rotational level, and $F(J)$ = energy of Jth rotational level from the 0th rotational level. $F(J)$ is given by

$$F(J) = BJ(J+1) - DJ^2(J+1)^2,$$

with $D \ll B$.

Then the net optical gain coefficient for a rotational transition between vibrational levels 1 and 2 can be shown to be[3]

$$\alpha_{1_J 2_{J\pm 1}} = \left(\frac{\ln 2}{\pi}\right)^{1/2} \frac{16\pi^3 c^3}{3h\Delta\nu_D \lambda_{1_J 2_{J\pm 1}}} \left|\sum R^{1_J 2_{J\pm 1}}\right|^2 \times \left(\frac{N_{1_J}}{g_J} - \frac{N_{2_{J\pm 1}}}{g_{J\pm 1}}\right), \qquad (2)$$

assuming that the transitions $1_J - 2_{J\pm 1}$ are primarily Doppler broadened, and where

$$\left|\sum R^{1_J 2_{J\pm 1}}\right|^2$$

is the matrix element[2] for the transition.

According to reference 2, $\left|\sum R^{1_J 2_{J\pm 1}}\right|^2$ can be split up into two parts, one which is dependent on J and the other which is independent of J; i.e.,

$$\left|\sum R^{1_J 2_{J\pm 1}}\right|^2 = K_{12} S_J, \qquad (3)$$

where $S_J = J$-dependent part of the matrix element, and K_{12} is that part of the matrix element which does not depend on J. $S_J = J+1$ for the P branch, and $S_J = J$ for the R branch, where J is the rotational quantum number of the upper level.

Then substituting Eq. (1) in (2), with

$$\Delta\nu_D = \lambda_{1_J 2_{J\pm 1}}^{-2} [(2kT/M)\ln 2]^{1/2},$$

where M = molecular mass, we obtain (a) for P-branch transitions, i.e., for $P(J+1)$,

$$\alpha_{1_J 2_{J+1}} = \frac{8\pi^3 c^4 K_{12}}{3kT}\left(\frac{2\pi kT}{M}\right)^{1/2}(J+1) \times \left\{N_1 B_1 \exp\left[-F_1(J)\frac{hc}{kT}\right] - N_2 B_2 \exp\left[-F_2(J+1)\frac{hc}{kT}\right]\right\}, \qquad (4)$$

and (b), for the R-branch, i.e., $R(J-1)$ transitions,

$$\alpha_{1_J 2_{J-1}} = \frac{8\pi^3 c^4 K_{12}}{3kT}\left(\frac{2\pi kT}{M}\right)^{1/2} \times J\left\{N_1 B_1 \exp\left[-F_1(J)\frac{hc}{kT}\right] - N_2 B_2 \exp\left[-F_2(J-1)\frac{hc}{kT}\right]\right\} \qquad (5)$$

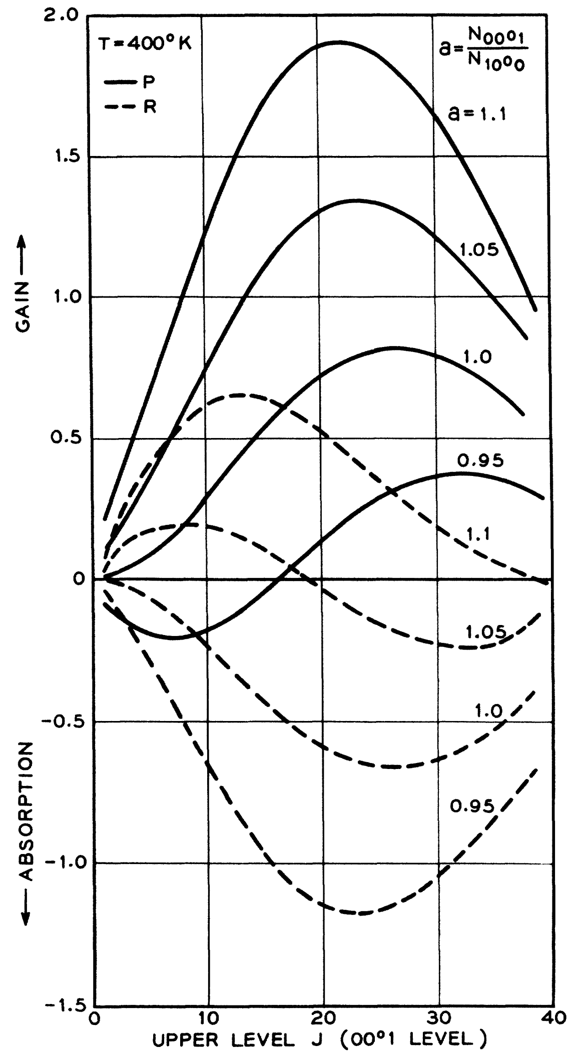

FIG. 2. Normalized gain as a function of upper-level J for P and R branches (for $T = 400°$K and $N_{0\,0^01}/N_{1\,0^00} = 0.95$, 1, 1.05, and 1.1).

The gain coefficients calculated from Eqs. (4) and (5) for $0\,0^01$ as the upper level and $1\,0^00$ as the lower level are plotted in Fig. 2 as a function of upper level J. $T = 400\,°$K has been assumed and should be reasonable for a gas discharge. The curves are given for various values of $N_{0\,0^01}/N_{1\,0^00}$ and are arbitrarily normalized to

$$\frac{8\pi^3 c^4 K_{12}}{3kT(2\pi kT/M)^{1/2}} N_2.$$

($B_{0\,0^01} = 0.3866$ cm^{-1}, $B_{1\,0^00} = 0.3897$ cm^{-1}, and $B_{0\,2^00} = 0.3899$ cm^{-1}).

From Fig. 2 the following conclusions can be reached immediately:

(a) P-branch transitions show optical gain even when $N_{0\ 0^01}/N_{1\ 0^00} < 1$, i.e., when the total population density in the lower vibrational level exceeds that in the upper vibrational level.

(b) R-branch transitions show gain only when $N_1/N_2 > 1.02$ for $T = 400\,°\text{K}$.

(c) R-branch transitions have lower optical gain than that for the P-branch transitions starting from the same upper level J.

Similar conclusions can also be reached for the $0\ 0^01$-$0\ 0^02$ band without actual calculations since the $B_{1\ 0^00}$ and the $B_{0\ 2^00}$ are very nearly equal.

The agreement between theory and experiment on the CO_2 maser experiments may be seen in Fig. 3. The $0\ 0^01$-$1\ 0^00$ band oscillates on P transitions from $J = 11$ to $J = 37$ (upper-level J's are used). The strongest transition is that for $J = 23$ and is also shown in Fig. 3. The best fit as can be seen is obtained for $N_{0\ 0^01}/N_{1\ 0^00} = 1.05$. (The fit is regarded as good when the two extreme oscillating transitions have the same optical gain and the peak of the gain curve coincides with the strongest optical-maser transition.) The lower curve in Fig. 3 shows the best fit for the $0\ 0^01$-$0\ 2^00$ transitions which oscillate for $J = 21$ to $J = 33$ with the strongest transition

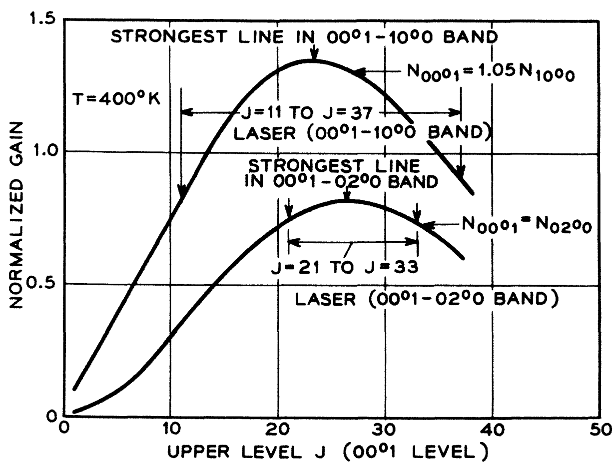

FIG. 3. Normalized gain as a function of upper level J for P branch (for $T = 400\,°\text{K}$ and $N_{0\ 0^01}/N_{1\ 0^00} = 1.05$, $N_{0\ 0^01}/N_{0\ 2^00} = 1$), together with observed laser transitions and strongest laser lines.

occurring for $J = 27$. Here for best fit, $N_{0\ 0^01}/N_{0\ 2^00} = 1.0$ is required. Thus for the best fit, we have $T = 400\,°\text{K}$, $N_{0\ 0^01} = N_{0\ 2^00} = 1.05 N_{1\ 0^00}$. It should be noted here that absolute value of gain depends upon K_{12} which is not the same for the $0\ 0^01$-$1\ 0^00$ and $0\ 0^01$-$0\ 2^00$ bands. And hence the apparent difference between the oscillation threshold gain for $0\ 0^01$-$1\ 0^00$ and that for $0\ 0^01$-$0\ 2^00$ bands, as seen in Fig. 3, is not significant.

Going back to Fig. 2 it can be seen that for $N_{0\ 0^01}/N_{1\ 0^00} = 1$ (or also for $N_{0\ 0^01}/N_{0\ 2^00} = 1$), the R branch does not show optical gain and hence it is quite easy to understand why the R transitions in the $0\ 0^01$-$0\ 2^00$ band do not oscillate. For $N_{0\ 0^01}/N_{1\ 0^00} = 1.05$ we see that the R-branch transitions do show optical gain for low J values, but in all cases, the gain on R transition is lower than that for a P-branch transition starting from the same upper J level. Thus due to competition effects, the P transition will oscillate preferentially. Consequently the populations in 1_J and 2_{J+1} levels will equalize and this will cause a further reduction in the gain on the R transition (i.e., population inversion between 1_J and 2_{J-1} levels). Hence, it is not too surprising to find that R transitions have not been seen in maser oscillation for $0\ 0^01$-$1\ 0^00$ band also. (The last argument holds only in the case when there is no wavelength discriminating device present in the optical-maser cavity to differentiate between λ_R and λ_P. This was the case for the maser experiments reported in reference 1.)

We would like to thank Dr. C. G. B. Garrett, Dr. J. P. Gordon, and Dr. P. K. Tien for critical comments and suggestions on the manuscript.

---

[1]C. K. N. Patel, W. L. Faust, and R. A. McFarlane, Bull. Am. Phys. Soc. 9, 500 (1964).

[2]G. Herzberg, Molecular Spectra and Molecular Structure II, Infrared and Raman Spectra of Polyatomic Molecules (D. Van Nostrand and Company, Inc., Princeton, New Jersey, 1945).

[3]A. C. G. Mitchell and M. W. Zemansky, Resonance Radiation and Excited Atoms (Cambridge University Press, New York, 1961).